Proceedings World Geothermal Congress 2020+1
Reykjavik, Iceland, April - October 2021

Numerical Pressure Transient Analysis of a Low Permeability Well with Water Hammer Effects during Injection Fall-off Test: Belgium Case Study

Azhari S. Adiputro[1], Sadiq J. Zarrouk[2]*, Richard J. Clarke[2], Virginie Harcouët -Menou[3] and Stijn Bos[3]

[1] Ulubelu Field, PT. Pertamina Geothermal Energy, Jakarta, 10340, Indonesia

[2] Department of Engineering Science, The University of Auckland, Private Bag 92019, Auckland, New Zealand

[3] VETO NV, Boeretang 200, 2400 Mol, Belgium

*s.zarrouk@auckland.ac.nz

Keywords: Deep geothermal well, fractured reservoir, PTA, numerical model, injection fall-off test, fractional dimension, water hammer.

ABSTRACT

Deep geothermal wells and geothermal wells targeting naturally fractured/fissured reservoirs often encounter low matrix permeability in the target reservoirs (pay zone). In some cases, extended pressure fall-off data of such wells display oscillations that cannot be easily interpreted by using the existing analytical pressure transient analysis (PTA) methods. Additionally, water hammer effects resulting from the shutting off the well are sometimes observed immediately after valve closure.

A new numerical PTA framework using the TOUGH2 simulator (Pruess, Oldenburg, & Moridis, 1999) was developed to analyse wells with such a typical behaviour. The approach was applied to a case study in Belgium (well MOL-GT-03) for which extended injection-fall-off well test data were analysed. A 1-D numerical radial model with a fractional dimension (fractal) grid structure was set up. A PyTOUGH script (Croucher, 2011) was written for correcting the measured wellhead pressure field data to reflect reservoir conditions and for automating the models running and historical data matching (during the injection and fall-off stages).

For well MOL-GT-03 the good match between the fractional dimension numerical model and the field data clearly indicated that the low reservoir permeability is dominated by small fractures and not rock matrix permeability. In addition, the water hammer effect (appearing as a sinusoidal wave) visible during the first 90 seconds after shutting down the injection test master-valve (very beginning of the pressure fall-off) was investigated by solving the wave equation. This new approach helps identify the extent of the well reach and provides a new estimate to the distance between the well and the reservoir boundary.

1. INTRODUCTION

Pressure Transient Analysis (PTA) is a standard tool in the petroleum and ground water industries to analyse a well test dataset. Estimated permeability, wellbore storage, and wellbore skin can be obtained. PTA can also be used to identify reservoir boundaries. PTA is commonly used in geothermal well test analysis of injection fall-off tests. However, the conventional PTA, which based on analytical models of the diffusion equation, does not commonly match geothermal well test datasets (McLean & Zarrouk, 2015a). Numerical PTA is then developed to give more understandings of the geothermal well test (McLean & Zarrouk, 2017b). Table 1 lists few numerical model implementations when analysing several well test data.

Table 1. Summary of numerical model implementation for different phenomena

Phenomena	Numerical model implementation	Results of the numerical model	References
Presence of linear impermeable boundary in the reservoir	1-D radial model. Modification of volume and contact area between blocks.	Similar response to analytical model equivalent.	McLean & Zarrouk (2015c)
Presence of a channel in the reservoir	1-D radial model. Modification of volume and contact area between blocks.	Produced the same plot as analytical PTA but different result. Analytical PTA overestimates the skin.	McLean & Zarrouk (2017a)
		Good match with a narrow channel reservoir model — approximate 5m width.	McLean et al. (2018)
Fractured formation during the injection-fall-off test	3-D grid model with horizontal and vertical fracture model.	Vertical fracture model gives a perfect match with data.	Bakar & Zarrouk (2018)

In this work, an unusual injection/fall-off pressure response data from a deep geothermal well are analysed. The pressure fall-off data shows multiple oscillations (Figure 1 left), which cannot be interpreted using analytical PTA. Furthermore, the sinusoidal pressure wave (water hammer effects) shows in the very early fall-off time (Figure 1 right).

In order to analyse this deep geothermal well behavior during the injection fall-off test, new numerical PTA framework is applied (McLean and Zarrouk, 2017b). The injection fall-off and water hammer will be analysed separately. Injection/fall-off pressure data oscillation will be analysed using a 1-D radial model combine with the fractal dimension model, to represent changing fracture

behavior, using the TOUGH2 simulator. While the water-hammer effect will be analysed using the wave equation in a numerical simulator COMSOL Multiphysics®. The water hammer data analysis is anticipated to provide additional information about the geothermal reservoir.

Two different methods are used to analyse injection/fall-off and water hammer effect. The model set up follows the numerical modelling framework (McLean & Zarrouk, 2017b) and is modified by adding a fractional dimension (Barker, 1988). The model then runs in the subdivided time interval and the parameters are adjusted to match the field data. The model parameters are then analysed after the best possible match is achieved. The water hammer data are set in COMSOL Multiphysics® numerical simulator with actual well geometry. The wave equation is used for the governing equation. The model then runs with the time-dependent simulation. The model parameters are adjusted to match the field data until the best possible match is achieved. The model parameters are then presented and discussed.

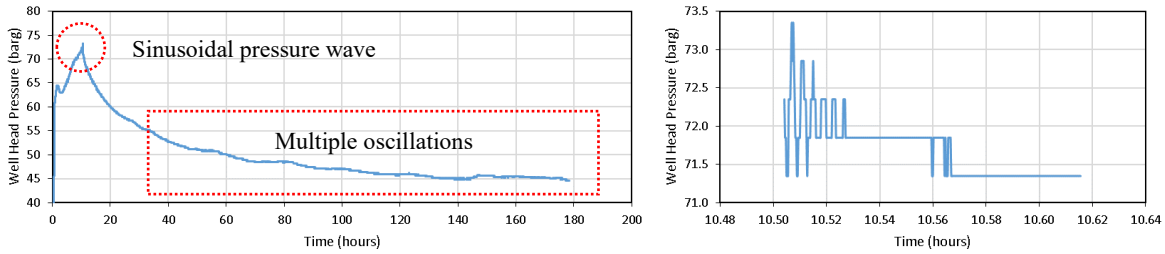

Figure 1. Multiple oscillations at fall-off data (left) and sinusoidal pressure wave (right) at well MOL-GT-03

2. NUMERICAL MODEL FOR THE INJECTION/FALL-OFF TEST

2.1 TOUGH2 Radial Model Setup

The numerical model, which is used in this study, is the 1-D radial model. This model's geometry design consists of a well and a single layer reservoir with a logarithmically spaced radial grid, as shown in Figure 2.

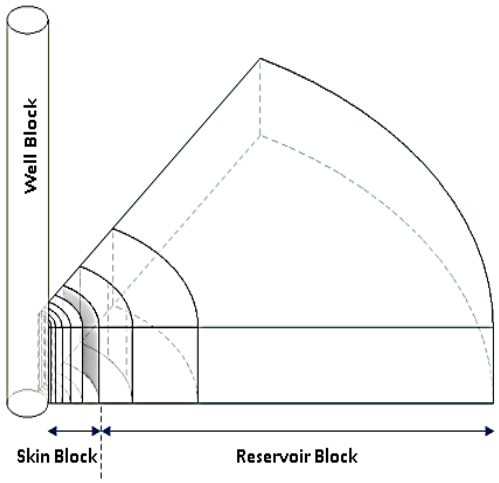

Figure 2. The design of the 1-D radial model and logarithmically spaced radial grid along the model.

2.1.1 The 1-D Radial Model Setup

The model has a default parameter that refers to the numerical modelling framework for pressure transient analysis of geothermal wells (McLean & Zarrouk, 2017b). Some parameters have been modified based on well MOL-GT-03 geometry data (asterisk* in the table). Selected parameters will be adjusted to match the model result and the field data. The model default parameters are shown in Table 2.

Table 2. The default 1-D radial model parameters

Parameters and description	Default model value
Total number of radial blockst	500
Number of blocks in the skin zone	158
Number of blocks in the reservoir zone	342
Model radial extend (km)	20
Layer thickness (m): from the total depth of perforated liner zone*	1155
Well radius (m): from the hole diameter (8 ½ in) of perforated liner zone*	0.108

Well permeability (D)[1] : 3 order of magnitude of default k_r	10
Well porosity: constant	0.9
Well volume (m^3): total of well volume*/0.9	34.6
Well block compressibility (Pa^{-1})	6×10^{-8}
Skin zone radius (m)	5
Skin zone permeability (mD)	10
Skin zone porosity : constant	0.1
Skin factor	0
Reservoir zone permeability, k_r (mD)	10
Reservoir zone porosity: constant	0.1
Maximum numerical timestep (s)	100
Equation of State (EOS)	EOS1

The total number of blocks is adjusted to be 500 blocks. The well MOL-GT-03 is predicted to have a very tight (low) reservoir permeability due to the slow pressure falloff, and having more blocks near the well will help the near well matching process. Furthermore, McLean & Zarrouk (2017b) explained that the number of blocks has no sensitivity to the model result. The TOUGH 2.2 EOS1 (water and energy) is used because the well is full of water up to the wellhead with no reported free gas. The adjustable parameters for the matching process from Table 2 above are the number of blocks in the skin zone (or skin zone radius), number of blocks in the reservoir, skin zone permeability, and reservoir permeability.

2.1.2 Fractional Dimension (Fractal) Model

Barker (1988) studied the mathematical solution for the generalised radial flow model of hydraulic testing in fractured rock. Barker (1988) showed that: the flow in fractured media does not necessarily have to be an integer number of dimension. The dimension can be fractional with the number somewhere between one, two, and three dimensions. Barker (1988) described that the one-dimensional flow is from a plane, the two-dimensional flow is from a uniform cylindrical porous media and the three-dimensional flow is from a spherical porous media. The author derived the mathematical equation in order to modify the area and volume to represent the fractional dimension model.

Zarrouk et al., (2007) utilised the generalised radial flow model to match the production data from the Poihipi dry steam zone which is part of the Wairakei geothermal field. Zarrouk et al., (2007) embedded the calibrated radial blocks into a three-dimensional reservoir non-structured grid model to represent the near well fracture controlled flow. The blocks volume and contract area between the radial blocks were modified to represent the fractional dimension model. The result showed that the fractional dimension model gives the best fit to the field test data. Furthermore, Zarrouk et al., (2007) concluded that using a fractional dimension model is simpler than other models that requires a large number of blocks.

2.1.3 Injection Parameter

There are two input parameters for the injection part of the well test, which are the flow rate and the injected water enthalpy. The flow rate is obtained from the field data during the injection process, while the enthalpy is calculated from the injection temperature. The injected water flow rate is measured at the wellhead while the injection temperature for the 1-D radial model should be located in the middle of the 'pay zone' (reservoir layer thickness). This leads to the difficulty of estimating the right injection temperature that can be used for the 1-D radial model. This is when McLean & Zarrouk (2017) clearly demonstrated that the cold injection temperature has a significant impact on the analytical pressure derivatives that can mistakenly be interpreted as positive skin. In this study, a new approach will be used to calculate the approximate injection temperature at the reservoir depth. To do that, the temperature of the well block will be investigated along the injection period and pressure fall-off time.

2.2 Well Block Temperature at Reservoir Depth

Since the well test data (injection water temperature and Pressure) are measured at the wellhead. The well-block fluid temperature at pay zone (reservoir) depth is required to find the correct enthalpy of injected fluid for the TOUGH2 input data. This is also to correct the pressure history (recorded at the wellhead), whereas the model needs pressure at reservoir depth.

Well MOL-GT-03 geophysical logs was used to estimate the temperature profile for the well (Figure 3a), by knowing the bottom hole temperature. This temperature profile predicted to be decrease during the injection period as the result of cold-water injection at the top of the well, but should start to increase once injection stops during the pressure fall-off period. The multilayer radial model in TOUGH2 is built to simulate the change of the temperature.

2.2.1 Multi-Layer Radial Model Setup

The multilayer radial model in TOUGH2 is designed and built to investigate the temperature profile at the well block located at the reservoir depth. The model design is a multilayer radial model, as shown in Figure 3b. The model consists of 10 vertical layers and 100 horizontal blocks (logarithmically spaced radial block) for each layer. This model not only represents the well, skin zone, and reservoir zone but also represents the casing and rocks above the reservoir that have no permeability. The details of the model parameters setup are given in Table 3.

[1] The terms permeability refers to rock matrix permeability. Unless it is clearly stated fracture permeability, the terms permeability always refers to rock matrix permeability.

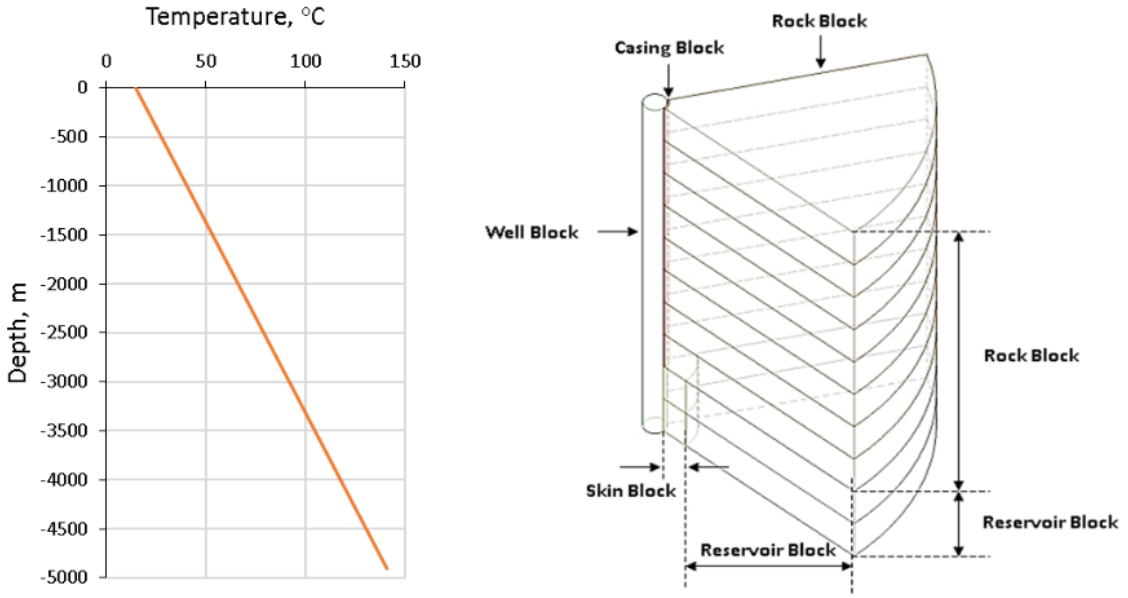

(a) (b)

Figure 3. (a) The estimated full warm-up temperature profile of well MOL-GT-03 (b) multilayer radial model used to calculate the injected fluid temperature at the reservoir depth.

Table 3. The multilayer radial model setup used to correct injected reservoir temperature.

Parameters and description	**Value**
Total number of blocks: constant	100
Number of layers	10
Layer thickness (m)	500
Model radial extend (km)	20
Number of the well block in each layer	1
Well permeability (m^2) *k1, k2, k3* (block a1 to a8)	10^{-30} , 10^{-30}, 10^{-11}
Well permeability (m^2) *k1, k2, k3* (block a9 to a10)	10^{-11}, 10^{-11}, 10^{-11}
Well porosity: constant	0.9
Well radius (m): average radius calculated from top to bottom	0.142
Number of casing block in each layer (layer 1 – 8)	3
Casing permeability (m^2)	10^{-30}
Casing specific heat (J/kg/K)	490
Casing conductivity (W/m/K)	52.92
Number of rock block in each layer (layer 1 – 8)	96
Rock permeability (m^2)	10^{-30}
Number of blocks in the skin zone (layer 9 and 10)	10
Number of blocks in the reservoir zone (layer 9 and 10)	90
Skin and reservoir zone permeability, k_r (m^2)	10^{-15}
Skin and reservoir zone porosity: constant[2]	0.1
Maximum numerical timestep (s)	100
Equation of State (EOS)	EOS1
Injection flowrate (kg/s) : 241 l/m at 15 degC injection water	4.02
Injection temperature at block a1 (°C)	15

The model attempts to represent the real condition of the well, which has reservoir blocks (including skin blocks), impermeable rock blocks above the reservoir, the well blocks from the surface up to the reservoir, and the casing blocks. The casing blocks and rock blocks are set to be impermeable to make sure the flow of the water only flows into the reservoir zone. The casing block's specific heat and heat conductivity are also set to represent carbon steel property.

The injection water enters the system at block a1 (on top of most of the well blocks) and the injection temperature result obtained at the block a9 (well block located at the reservoir depth). Block a9 is chosen because the reservoir midpoint from the top of the well is

[2] The porosity used in the model is based on the numerical PTA framework (McLean & Zarrouk, 2017b). However, in a low permeability well, the porosity could be lower. Changing this parameter will not change the result significantly.

at 4327.5 metres, and block a9 covers the depth between 4000 metres to 4500 metres. The initial static temperature uses the temperature profile of Figure 3a.

2.2.2 Temperature Profile and Field Data Pre-processing

The temperature profile of block a9 during injection is shown in Figure 4 left. The temperature profile of fall-off period has a rising trend as a function of time, as shown in Figure 4 right. After getting the temperature profile for the well block (block a9) during the injection period, the next step is to calculate the enthalpy, which will vary with time, and use this data as the TOUGH2 input enthalpy to run the 1-D radial model.

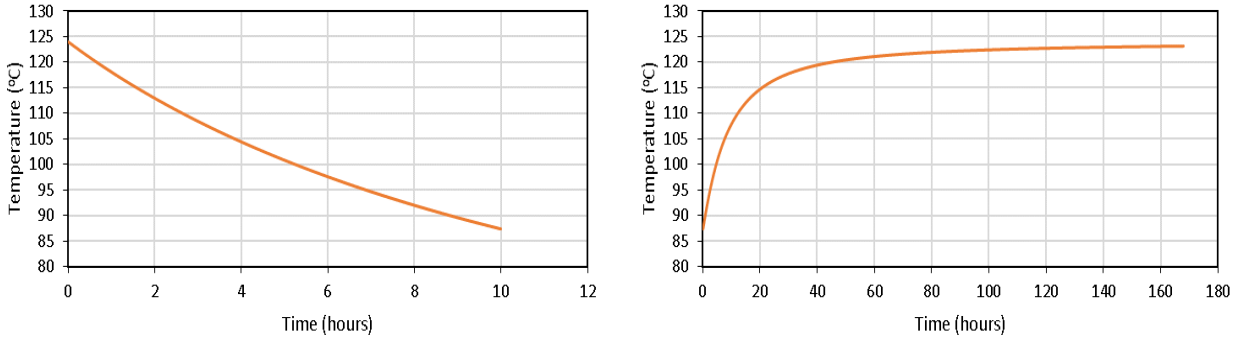

(a) (b)

Figure 4. (a) Temperature profile at bottom well block (a9) during the injection period, (b) Temperature profile at bottom well block (a9) during fall-off period.

In order to estimate the pressure at the reservoir, the geometry and temperature profile injection/fall-off are used for the calculation. The reservoir pressure is the sum of hydrostatic pressure in each well block from a1 to a9, plus wellhead pressure and atmospheric pressure. The temperature varies with time, resulting in the density of water becoming the function of time. Equation (1) expresses the calculation of the reservoir pressure for the specific time (every 1 second).

$$P_{res\,(bara)} = P_{atm} + P_{wellhead} + \sum_{i=1}^{9} \rho(T_i) * g * z \quad \begin{cases} z = 500m\ for\ layer\ 1\ to\ 8 \\ z = z_{res} - 4000m\ for\ layer\ 9 \end{cases} \tag{1}$$

where *i = model layer, P = pressure, ρ = density, z = depth*

2.3 Model and Field Data Matching

Before running the 1-D radial model, the reservoir pressure dataset is divided into several subsections. The reservoir pressure data will be matched with the 1-D radial model results in each (piecewise) subsection. For each subsection, the 1-D radial model parameters are adjusted to get the match. The adjustable parameters are the skin zone radius, skin zone permeability, reservoir zone permeability, and the fractional dimension (*n*).

In the first subsection, the dimension is fixed to a default value of 2, and the skin zone radius is set to be 5 metres for the first attempt. For the next subsections, the fractional dimension is adjusted to get the match. Next, after the result matches for a particular subsection, it will become the initial condition for the next subsection and so on. This process will continue until all subsections for the injection duration is completed. Then, the first subsection of fall-off is run using the same modeling criteria and initialisation. The parameters are adjusted until the reservoir pressure is fully matched. If there is a change in the reservoir permeability (k_r) at any stage, the model is re-run with the new permeability from the start of water.

Interestingly the modeling experiments found that the full pressure response could not be matched by changing the reservoir permeability only. Hence, it is assumed that the reservoir permeability is constant throughout the test. The parameters that were allowed to change are the skin zone permeability, skin zone radius, and the fractional dimension (n), which represents the fracture. This effectively gives the reservoir rock a fracture permeability. Figure 5a shows a very good match between the field data and 1-D radial model results for injection section, while Figure 5b shows a good match during pressure fall off.

In the fall-off section, the 1-D radial model is run per subsection. In order to get a match between the field data and model results, the model parameters are adjusted. The parameter that mainly changes is the dimension (*n*). There is a change in the skin radius at the beginning of the fall-off, but for the rest of the simulation, it is constant. The data matching did not only cover the pressure history plot but mainly the pressure derivative on the log-log plot (Figure 6a). Figure 5b shows that the model and field data have a good match in the pressure history plot. The model can nicely follow the pressure oscillation in the field data.

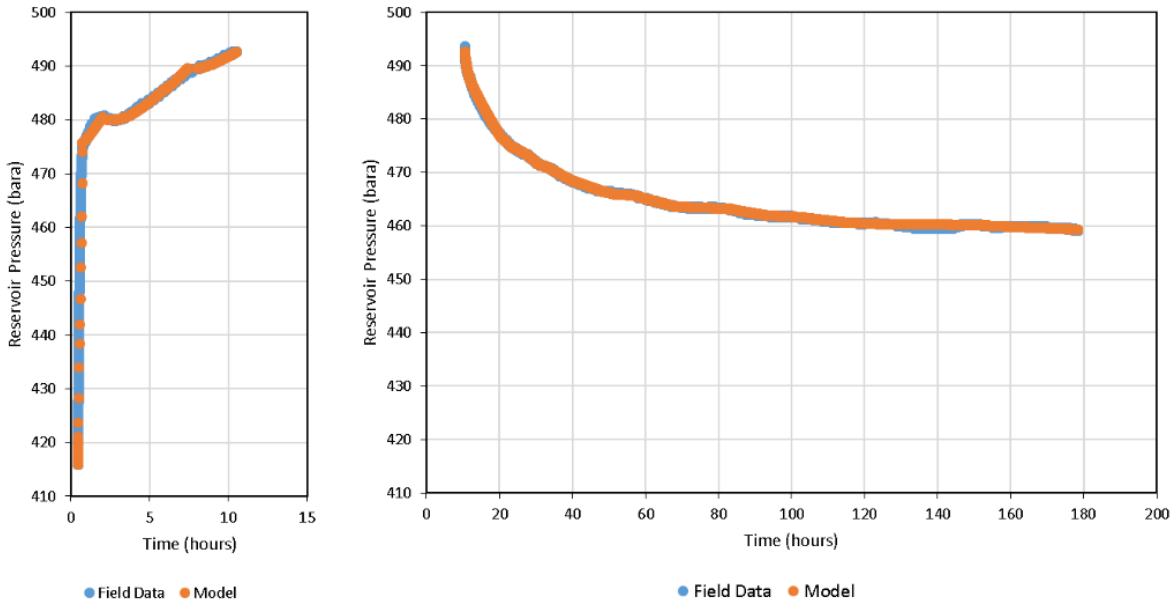

(a) (b)

Figure 5. (a) Pressure plot of model and field data, injection (left) and fall-off (right)

The delta pressure (dP) and pressure derivative (dP') plot for both model and field data are shown in Figure 6a. Figure 6a shows that the model and field data have a good match after dt = 1 hour (wellbore storage effect). The pressure oscillation during falloff is shown more clearly in the pressure derivative plot. The model shows that it can also match the pressure oscillation behaviour; such match is not possible using analytical models (Zarrouk and McLean, 2019). The scattered data, which is shown in the early time (Figure 6a), occurs because of the water hammer effect that has a sinusoidal pattern. This phenomenon cannot be simulated by a 1-D radial model in TOUGH2 and will be investigated using a different approach (Section 3).

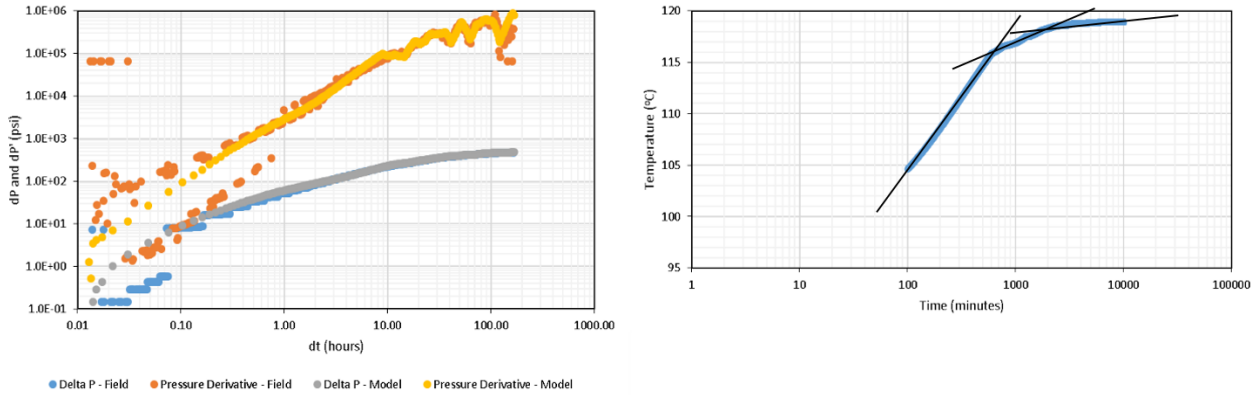

(a) (b)

Figure 6. (a) Fall-off pressure derivative and delta pressure plot of model and field data (Well MOL-GT-03), (b) temperature recovery in semi-log plot 100 minutes after fall-off.

During pressure fall-off, the temperature of the well block will recover to the initial condition. The semi-log plot of the temperature recovery from the 1-D radial model is shown in Figure 6b. The temperature profile can be fitted with a piecewise liner fit. This response of the temperature indicates the fracture permeability (Dunstall, 1992). However, the response cannot be observed immediately, but after 100 minutes of the fall-off test. It indicates that the reservoir has a micro fractures. These micro fractures manage to be open a little bit by the injection water. However, after the injection water stops, these fractures start to close.

2.4 Model Results

Figure 7 shows the fractional dimension (n) plot with time during both injection and fall-off parts of the test for the pressure match results given in Figures 5 and 6. The graph shows that during the injection period the dimension (n) decreases first, going down from the default start value of 2 to the lowest value of 1.7 at the end of the injection period. The sudden drop of pressure observed in the

pressure versus time plot corresponds to the sudden drop of n (from n = 2.1 to n = 1.86). This condition indicates that during the injection period the injection water is opening the fractures (formation breakdown) in the reservoir rock and the fluid flow in the reservoir is changing from the initially radial flow (n = 2) to be more like linear pipe (fracture) flow (n → 1).

During pressure fall-off, the fractional dimension (n) remains constant for the first 10 hours then starts to increase. The dimension (n) is increasing from 1.7 at the beginning of the fall-off period to 2.5 at the end of the test, along the fall-off period. Figure 7 shows that the n value is sometimes going up and down. This behaviour is corresponding to the wide pressure oscillation that shows up in the pressure history plot. The dimension (n), which is going up to the value of more than 2, indicates that the reservoir is changing from originally being between linear pipe/fracture flow and radial flow to be more of a the spherical symmetric reservoir.

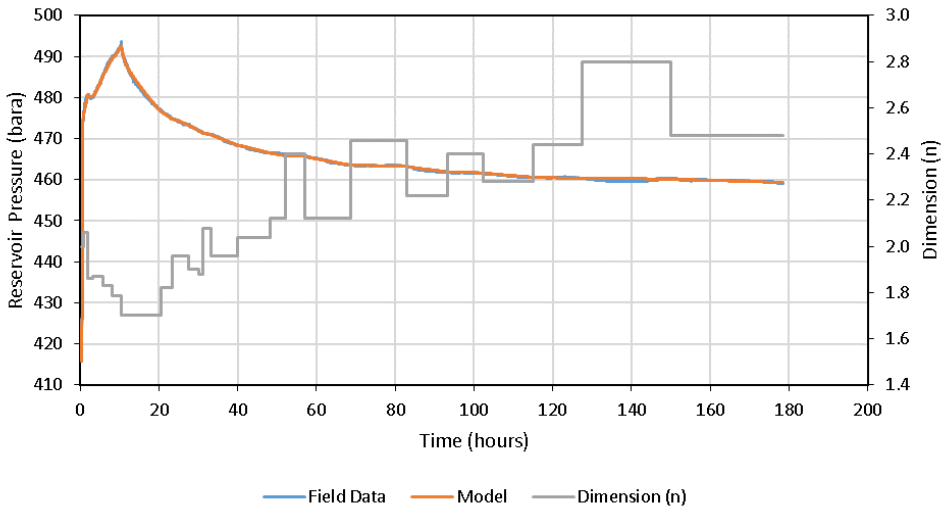

Figure 7. Dimension (n) plot versus time during the injection and fall-off test.

The reservoir permeability remains constant at 0.0018 mD or 1.8 µD from the beginning of injection to the end of the fall-off. This reservoir can be categorised as a tight reservoir (Zarrouk & McLean, 2019). The skin zone permeability is higher than the reservoir zone permeability. It also has a constant value during injection and fall-off of 0.0382 mD or 38.2 µD. This is common in geothermal reservoirs, which commonly have negative skin due to fracturing.

The reservoir permeability above is based on the assumption that all open sections of the well is part of reservoir thickness. However, in reality, the permeable zone could be smaller. In other words, there could be a permeable zone in a particular depth which has higher permeability and a non-permeable zone which has much lower permeability. Further investigation is needed to observe the location of the permeable zones such as the data from the spinner tool and drilling penetration rate would be needed (Zarrouk and McLean, 2019). Hence, in this work, the permeability is assumed to be the average permeability for open section (not cased) of the reservoir thickness.

2.5 Discussion

The multilayer radial model can be used to calculate the injection temperature profile with extended fall-off temperature profile. As predicted by McLean & Zarrouk (2015b) the temperature is non-uniform, time-varying, and located in-between injected temperature and reservoir temperature. The multilayer radial model demonstrates the ability not only for estimating the approximate temperature profile but also for correcting the pressure history data from the wellhead to the reservoir conditions.

Modelled pressure derivative plots has a very good match with their corresponding well test data. The dimension (n) decreasing profile clearly shows that the fracture opening due to injection water. The fluid flow is changing from radial flow (n = 2) to be more likely fracture flow (n = 1), which results in the dimension value between one and two. The injection water manages to open (widen) existing small fractures, and the fluid flows into these fractures.

The fracture permeability is also confirmed by the transient fall-off temperature profile on the semi-log plot. The temperature profile clearly shows that the piecewise straight line fit that occurs in the well with has fracture permeability. However, the effect of this temperature cannot be seen directly at the early fall-off time, but is clear in the later period, due to the small reservoir fractures. These micro fractures are opened by the injection water.

The up-down profile of dimension (n) has occurred in the fall-off period, with an overall increasing trend. The dimension up-down profile relates to the oscillating pressure response, which has occurred in its pressure history. The increasing trend of dimension in the fall-off indicates that the fluid flow is changing from the tendency to be fracture flow more into all directions in the spherical reservoir.

At the beginning of the pressure fall-off, the skin region is shrinking; in other words, the farthest part of the skin is changing in permeability to be tighter. In general, the well has a constant value of skin permeability and reservoir permeability during the injection fall-off tests.

3. NUMERICAL MODEL FOR WATER HAMMER EFFECT

3.1 Formulation

The water hammer effect is a hydraulic/fluid transient phenomenon. The equation can be derived from mass and momentum conservation. Acheson (1990) showed how the wave equation for pressure can be derived from mass conservation and momentum conservation. The resulting one-dimensional wave equation is shown in Equation. (2). Hence, with this approach, the wave equation can be used to simulate the water hammer, which originally derived from mass and momentum conservation. However, the classical wave equation is non-dispersive, so the wave will remain oscillating without attenuation.

$$\frac{\partial^2 p}{\partial t^2} = {\alpha_0}^2 \frac{\partial^2 p}{\partial x^2} \tag{2}$$

where α_0 is the speed of sound. This is the wave equation first derived by Euler in 1759.

Szabo (1994) derived a general lossy dispersive wave equation. With this equation, the wave attenuation is possible and complies with an empirical frequency power law. A study by Chen & Holm (2003) later modified the Szabo equation by including Caputo fractional derivative.

The numerical simulator COMSOL Multiphysics® is used in this study to simulate the water hammer effect with the wave equation as the governing equation. In order to accommodate the attenuation, a first order time derivative should be added into the classical wave equation (COMSOL Multiphysics®, 2012). This is in line with the wave equation by Chen & Holm (2003), which consists of the wave equation with additional first time derivative as the attenuation term (Equations 3 and 4).

$$\nabla^2 p = \frac{1}{{c_o}^2}\frac{\partial^2 p}{\partial t^2} + \frac{2\alpha_0}{c_0} Q_y(p) \tag{3}$$

$$Q_y(p) = \frac{\partial p}{\partial t}\,, \quad \text{for} \quad y = 0 \tag{4}$$

where c_0 is the speed of sound.

3.2 COMSOL Multiphysics® Implementation

Four different model geometries were tested including: 3D Disk Model, 2D T-Model, 3D T-Model, and 3D Vertical Model (Deepening Model).

The implementation starts with building the 3D model. The geometry will be described separately in each model. The coefficients for wave equation and boundary conditions are:

1. Wave equation, diffusion coefficient $c_1 = (1481)^2$, $c_2 = (4750)^2$, mass coefficient (e_a) = 1
2. Initial value, $p = 0$, $\frac{\partial p}{\partial t} = 0$
3. Zero flux all boundary, except overridden by dirichlet boundary
4. Dirichlet boundary condition (reservoir), $r = 0$
5. Dirichlet boundary condition (valve, $z = 0$ *m*)

$$P = \rho c u_0 \tag{5}$$

where,
average fluid velocity $u_0 = \frac{q_0}{\pi r^2}$; $\mathrm{q_0} = \text{injection rate (l/min)}$; $\mathrm{r} = \text{average well radius (m)}$

Different mesh size (*dx*) is used in different models. The CFL number is set to be 0.1. The boundary condition at the valve is changing from pressurized to zero flux in order to enable the reflection of the pressure wave. Hence, two separate simulations are used. The first simulation is run from t = 0 s to t = 0.03 s, while the second simulation is run from t = 0.03 s to t = 80 s. The result from the first simulation become the initial condition of the second run. In both, the time step is defined as $dt = \mathrm{CFL}*dx/c_1$ and the amplification for high frequency is 0.1.

3.3 Model Geometry and Results

3.3.1 The 3D Disk Model (without Attenuation Term)

A 3D model of the well and disk (wide cylinder) reservoir is built as illustrated in Figure 8. In this model, two different speeds of sound are used. The speed of sound (c_1) with a value of 1481 m/s is used for the well (full of water), and c_2 with a value of 4750 m/s is used for the reservoir (rock) region. The speed of sound in the rock corresponds to the average P-wave velocity for limestone given by Mavko (2005). The reservoir boundary condition is located at the side of the disk block. In this model, parameter disk radius (R) and disk thickness (T) will be varied to get the match.

The model results are compared to the model without a disk representing the reservoir to check the sensitivity of the disk radius and disk thickness. The result of the simulation is given for a point near the wellhead, located at z = 0.1 m below the well-head (top of the model). Figure 9 shows that neither the radius of the disk nor its thickness nor even the presence of the reservoir disk affects the simulation result. In this particular disk model, the pressure wave is not sensitive to the geometric parameters of the reservoir disk. This indicates that most of the reflected pressure wave originates from the bottom of the well, and that using a model without the reservoir disk is can provide the same results.

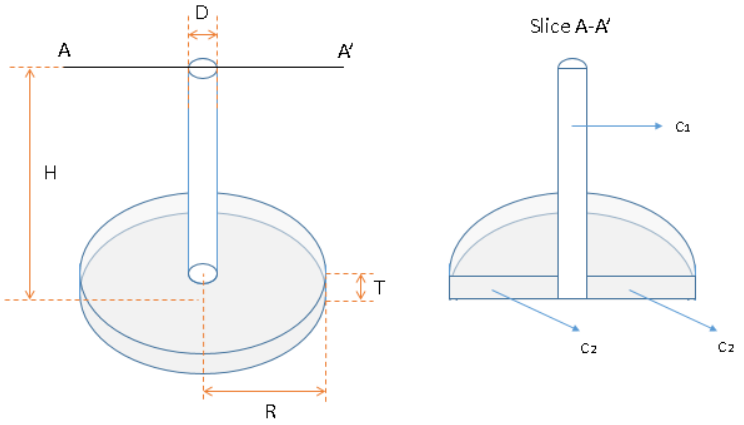

Figure 8. The 3D disk model illustration

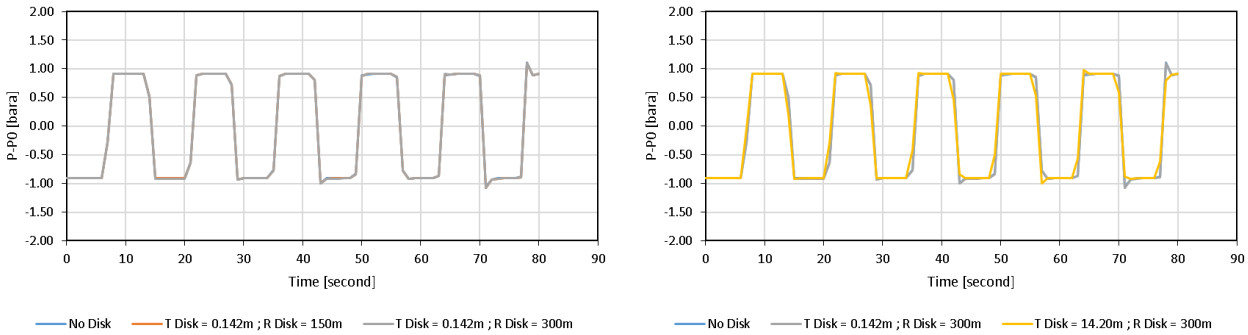

(a) (b)

Figure 9. The 3D disk model result with variation of disk radius (a) and disk thickness (b)

3.3.2 The 3D T-Model

The 3D T-Model is the three-dimensional equivalent to the 2D T-Model. Two scenarios were also investigated in 3D: the first model with c_1 in all regions and the other model with c_1 in the well region and c_2 in the reservoir region. Model geometry uses depth (H) of 4327.5 metres, well diameter (D) of 0.284 metres, and reservoir thickness (T) of 0.248 metres. The wave equation is implemented as the governing equation (3) with two dirichlet boundary conditions for the valve at the top of the model, and a dirichlet boundary condition of constant pressure at both ends of the horizontal pipe. Other boundaries are set to be no flux. The models are run and the results are compared to the field data. The adjustable parameters of the model are the reservoir radius (R) and attenuation term $2\alpha_0 c_0$. The 3D T-Model is illustrated in Figure 10 (left).

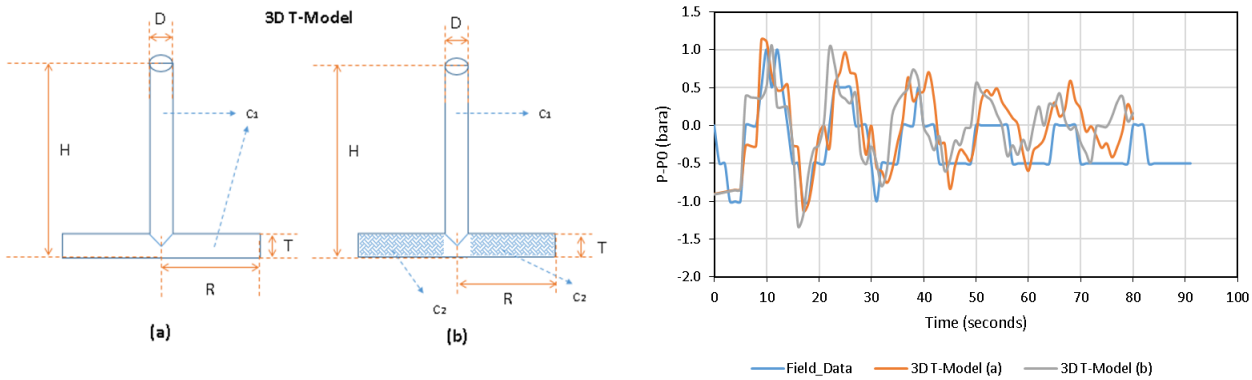

Figure 10. The 3D T-Model with c_1 in all-regions (a); 3D T-Model with c_1 in the well and c_2 in the reservoir region (b); results of 3D T-Model (right)

Figure 10 (right) shows the results of the 3D T-Models. The 3D T-Model (a) has a reasonable match with the field data as well as the 3D T-Model (b). However, in the late-time, the wave result tends to shift left for the 3D T-Model (b). For the model parameters, the 3D T-Model (a) uses R = 1.8 km while the 3D T-Model (b) uses R = 10 km. Both models also give the same $2\alpha_0 c_0$ value at about 0.33.

3.3.3 The 3D Vertical Model

Additional 3D Vertical Models where the well extends to greater depth have also been tested. The so-called 3D Vertical Model consists of 1) a vertical well with total well length H_1 (here 4905 m) and diameter D (0.248 m) and 2) a vertical extension section of thickness H_2 (to which either reservoir or well properties are attributed). Again, a matching exercise was performed. For the matching exercise, the adjustable parameter is parameter H_2 and $2\alpha_0 c_0$. The model is illustrated in Figure 11 (left).

Two models are built to accommodate the different speed of sound. One model has the speed of sound c_1 for all regions (a), while the second model has different speed of sound c_1 for the well region and c_2 for reservoir region (b). All boundaries are no flux boundaries except the dirichlet boundaries at the top of the well (as valve) and at the bottom of the well.

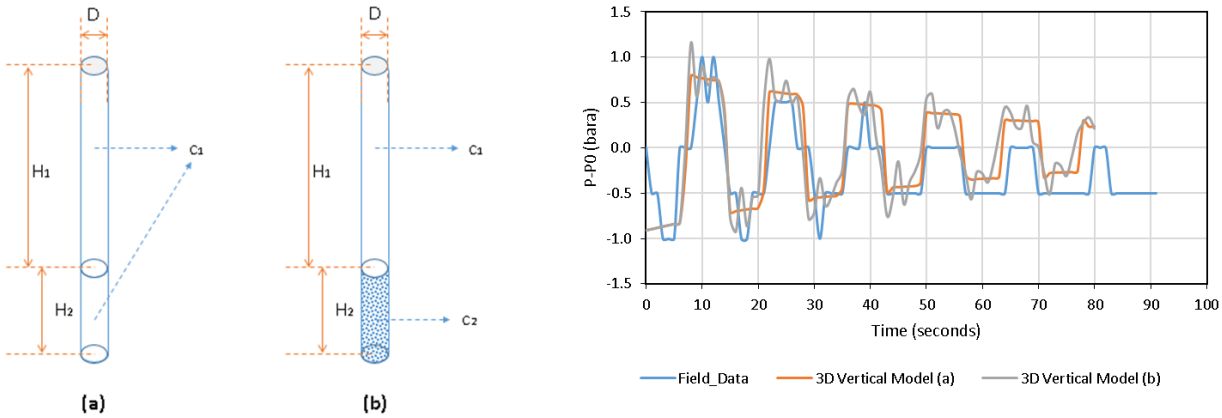

Figure 11. The 3D Vertical Model with c1 all-region (a); 3D Vertical Model with c1 at the well and c2 at the reservoir region (b); results of 3D Vertical Model (right)

Figure 11 (right) shows the results of both 3D Vertical Models. A fairly good match is achieved between the model results and the field data assuming that the model should extend H_2 = 300 m and H_2 = 2400 m deeper for 3D Vertical Model (a) and (b), respectively. Both models indicate that the best match is obtained with the same $2\alpha_0 c_0$ value at about 0.33. Table 4 summarises all the model parameters and matching results.

Table 4. Summary of model parameters and matching results

Models	Speed of sound (m/s)		Well depth (meter)	Reservoir thickness (meter)	Reservoir radius (meter)	Vertical extension (meter)	Lossy media constant	Results
	c_1	c_2	H or H_1	T	R	H_2	$2\alpha_0 c_0$	
3D Disk Model	1,481	4,750	4,905	0.142 14.20	150 300	-	-	The pressure wave cannot propagate horizontally in disk geometry. The model cannot be used to match the data.
3D T-Model (a)	1,481	-	4,327.5	0.248	1,800	-	0.33	Good match with field data
3D T-Model (b)	1,481	4,750	4,327.5	0.248	10,000	-	0.33	Good match with field data before t = 30 s, then the wave slightly shifts left
3D Vertical Model (a)	1,481	-	4,905	-	-	300	0.33	Good match with field data
3D Vertical Model (b)	1,481	4,750	4,905	-	-	2,400	0.33	Good match with field data

3.4 Discussion

From the results of the 3D disk model, this particular disk geometry model is not sensitive to the reservoir radius and thickness. The results obtained were the same as from the only vertical well model without disk reservoir geometry. The model indicates that the pressure wave does not have significant propagation amplitude for the horizontal distance into the reservoir. The major of the reflected wave comes from the contact point between the well and reservoir, which is equal to the vertical depth of the well. Hence, this model cannot be used to match the data.

Both 2D T-Model and 3D T-Model give similar good simulation result with the well test data. The simulation result can match with the field data frequency by adjusting the horizontal distance. The simulation indicates that the pressure wave is affected by the length of the horizontal geometry. On the other hand, the 3D Vertical Model gives a similar result to the T-Models. In this case, the simulation

result can match the field data frequency by adding the well depth. The lossy media approach which includes a first-time derivative term into the wave equation gave the best results. All models have the same result for the fitted parameter $2\alpha_0 c_0$.

The parameter α_0 could be related to the physical information at the well, rock, or even fractures shape/orientation. Further investigation is needed to correlate this parameter with the physical reservoir conditions. Additional information for further understanding could be obtained from geophysical surveys such as the spontaneous potential log, gamma ray log, porosity log, and resistivity log (Asquith & Krygowski, 2004). However, at the end, the model and field data have a reasonably good match by adjusting parameter $2\alpha_0 c_0$.

Regardless of the fact that some of the models may not be physically realistic, all parameters from the models which have a good match give proof that the pressure wave is propagating into the reservoir. The water hammer effect cannot produce the observed pressure wave by propagating within the well only. The pressure wave reflects from the reservoir back to the wellhead. Then, the wave travels back and forth and attenuates due to the loos medium it passes through or friction with the well casing. The wave could travel either to the bottom, which is modelled by 3D Vertical Model or to the side of the well, which is modelled by the T-Model. This could mean the reservoir is deeper than penetrated by the well or there is a fracture, respectively. Other physical explanations may also be considered in the future.

4. CONCLUSION

Several conclusions can be drwan from this study:

1. Sudden pressure drop in well MOL-GT-03 during injection test indicates fracture opening. The fluid flow is changing from radial flow into more like fracture flow with dimension parameter between 1 and 2.
2. The pressure oscillation behaviour in well MOL-GT-03 during the fall-off test correlates with dimension change and indicates the closing and opening of the fracture (fracture clapping). The increasing dimension trend indicates flow changing from fracture flow to all directions (tends to be more like the flow in the spherical reservoir).
3. Fractional dimension embedded inside the 1D radial model gives a perfect match to field test data.
4. Temperature warm-up of well MOL-GT-03 at fall-off indicates fracture permeability. However, the fracture is too small, so that the effect of temperature warm up cannot be observed in the early fall-off time.
5. The fractional dimension parameter is decreasing in the injection period associated with fracture opening because of injection water.
6. The multilayer radial model can be used as a new approach to approximate the reservoir temperature condition during injection and fall-off test. The results can be the input of injection temperature data for the 1D radial model and can be valuable information for correcting pressure data from wellhead to reservoir conditions.
7. Further study needed to simplify the re-creation of the temperature profile in each layer for multilayer radial model so the process will be less time-consuming.
8. The sinusoidal pressure wave pattern in the early fall-off indicates water hammer effect due to the sudden closure of the injection water valve. The wave travels through the well and reservoir until it hits a boundary and then reflected back to the wellhead. The wave will continue back and forth until all the energy is dispersed. It was proven that; the pressure wave need to go outside the well geometry to produce the observed water hammer effect.
9. A good match for T-Model is achieved by the model which uses the single speed of sound. However, in the Vertical Model, single speed of sound or a combination give a good match.
10. The T-Model result for well MOL-GT-03: horizontal distance length 1.8 km, for the assumption of the single speed of sound in water all across the region.
11. The Vertical Model result for well MOL-GT-03: additional vertical distance 300 m for single speed of sound and 2,400 m for a combination of speeds.
12. The developed numerical method can be used for other wells which have similar injection and fall-off pressure responses.

ACKNOWLEDGEMENT

The authors like to thank the management of VITO NV, Belgium for providing the geothermal well test data and the kind permission to publish the results.

REFERENCES

Asquith, G., & Krygowski, D. (2004). *Basic well log analysis* (Vol.16). Tulsa: American Association of Petroleum Geologist.

Bakar, H. A., & Zarrouk, S. J. (2018). Transient pressure analysis of geothermal wells fractured during well testing. *Geothermics*, *76*(June), 26–37. https://doi.org/10.1016/j.geothermics.2018.06.010

Barker, J. A. (1988). A generalized radial flow model for hydraulic tests in fractured rock. *Water Resources*, *24*(10), 1796–1804.

Chen, W., & Holm, S. (2003). Modified Szabo's wave equation models for lossy media obeying frequency power law. *The Journal of the Acoustical Society of America*, *114*(5), 2570. https://doi.org/10.1121/1.1621392

COMSOL Multiphysics. (2012). *COMSOL Multiphysics: User's guide*. US: Author.

Croucher, A. (2011). Pytough: A python scripting library for automating tough2 simulations. In *New Zealand Geothermal Workshop 2011 Proceedings* (pp. 1–6). Auckland, New Zealand.

Croucher, A. (2018). *PyTOUGH user ' s guide*. Auckland, New Zealand: The University of Auckland.

D. J. Acheson. (1990). *Elementary fluid dynamics*. New York, NY: Oxford University Press.

Dunstall, M. G. (1992). *Downhole heat exchangers performance analysis*. University of Auckland.

Mavko, G. (2005). *Conceptual overview of rock and fluid factors that impact seismic velocity and impedance*. *Stanford University*. Retrieved from https://pangea.stanford.edu/courses/gp262/Notes/8.SeismicVelocity.pdf

McLean, K., Mcdowell, J., Sepulveda, F., Seastres, J., Zarrouk, S. J., & Alcaraz, S. (2018). Upflow along a basement fault revealed by geothermal numerical pressure transient analysis. In *Proceedings 40th New Zealand Geothermal Workshop*. Taupo, New Zealand.

McLean, K., & Zarrouk, S. J. (2015a). Geothermal well test analysis using the pressure derivative: Some common issues and solutions. *Geothermics*, *55*, 108–125. https://doi.org/10.1016/j.geothermics.2015.01.010

McLean, K., & Zarrouk, S. J. (2015b). Linear impermeable boundary in geothermal pressure transient analysis : a reservoir modelling assessment. In *New Zealand Geothermal Workshop 2015 Proceedings*. Taupo, New Zealand.

McLean, K., & Zarrouk, S. J. (2017a). Geothermal reservoir channel located by pressure transient analysis: A numerical simulation case study. *Transactions - Geothermal Resources Council*, *41*.

McLean, K., & Zarrouk, S. J. (2017b). Pressure transient analysis of geothermal wells: A framework for numerical modelling. *Renewable Energy*, *101*, 737–746. https://doi.org/10.1016/j.renene.2016.09.031

Pruess, K., Oldenburg, C., & Moridis, G. (1999). *TOUGH2 users guide version 2.0*. *Earth Science Division, Lawrance Berkeley National Laboratory*. Retrieved from http://esd.lbl.gov/TOUGHPLUS/manuals/TOUGH2_V2_Users_Guide.pdf

Szabo, T. L. (1994). Time domain wave equations for lossy media obeying a frequency power law. *The Journal of the Acoustical Society of America*, *96*(1), 491–500. https://doi.org/10.1121/1.410434

Zarrouk, S., & McLean, K. (2019). *Geothermal well test analysis: fundamentals, applications and advanced techniques* (1st ed.). Academic Press.

Zarrouk, S., O'Sullivan, M., Croucher, A., & Mannington, W. (2007). Numerical modelling of production from the Poihipi dry steam zone: Wairakei geothermal system, New Zealand. *Geothermics*, *36*(4), 289–303. https://doi.org/10.1016/j.geothermics.2007.03.006